

Metal-Enhanced Multiphoton Absorption Polymerization with Gold Nanowires

Sanghee Nah,[†] Linjie Li,[†] Ran Liu,[†] Junjie Hao,[†] Sang Bok Lee,^{*,†,‡,§} and John T. Fourkas^{*,†,‡,§,||}

Department of Chemistry and Biochemistry, University of Maryland, College Park, Maryland 20742, Institute for Physical Science and Technology, University of Maryland, College Park, Maryland 20742, Maryland NanoCenter, University of Maryland, College Park, Maryland 20742, Center for Nanophysics and Advanced Materials, University of Maryland, College Park, Maryland 20742, and Graduate School of Nanoscience and Technology (WCU), Korea Advanced Institute of Science and Technology (KAIST), 335 Gwahangno, Yuseong-gu, Daejeon 305-701, Korea

Received: January 14, 2010

Metal-enhanced multiphoton absorption polymerization (MEMAP) is studied using gold nanowires with a set of three different photoresists. Photoresists that employ radical and cationic polymerization are investigated. In all cases, MEMAP is strongly correlated with multiphoton-absorption-induced luminescence (MAIL) of the nanowires. Wavelength-dependent studies indicate that the dominant mechanism for MEMAP is not field-enhanced two-photon absorption of the photoinitiator, but rather single-photon excitation of the photoinitiator by the broadband MAIL emission.

I. Introduction

Nanoscale objects composed of noble metals can enhance optical fields. Under appropriate circumstances, orders-of-magnitude enhancements are possible. Such field enhancements play a role in phenomena such as surface-enhanced Raman scattering (SERS),^{1,2} surface-enhanced infrared absorption (SEIRA),^{3–5} multiphoton-absorption-induced luminescence (MAIL)^{6,7} of noble-metal structures, and metal-enhanced multiphoton absorption polymerization (MEMAP).^{8–10}

The details of field-enhanced optical phenomena in noble-metal nanostructures are not yet fully understood. One approach that has been used recently to develop a deeper understanding of field-enhanced optical processes is to probe correlations among different phenomena in a single sample. For instance, we have reported a study on the relationship between the efficiencies of MAIL and MEMAP in aggregates of gold nanoparticles,¹⁰ and Mazur and co-workers have correlated the efficiencies of MEMAP and SERS on nanostructured silver surfaces.¹¹

While noble metals are not generally known for their luminescent properties, it was discovered more than 20 years ago that multiphoton absorption could lead to luminescence on noble metal surfaces, and that this luminescence was considerably stronger on rough surfaces than on smooth ones.⁶ MAIL has now been investigated for a wide range of noble-metal nanostructures, including nanoparticles,^{7,12–14} nanorods,^{15,16} nanowires,^{17,18} nanoshells,¹⁹ nanoplates,²⁰ and nanobowties.⁹ MAIL is also beginning to be used in biological imaging.^{19,21,22} Depending on the system studied, MAIL may involve the absorption of two or more photons of near-infrared light.¹⁸ The emission spectrum of MAIL can, in many cases, span the visible spectrum and extend into the ultraviolet and near-infrared.⁷

* To whom correspondence should be addressed. E-mail: fourkas@umd.edu; slee@umd.edu.

[†] Department of Chemistry and Biochemistry, University of Maryland.

[‡] Institute for Physical Science and Technology, University of Maryland.

[§] Maryland NanoCenter, University of Maryland.

^{||} Center for Nanophysics and Advanced Materials, University of Maryland.

^{||} Korea Advanced Institute of Science and Technology (KAIST).

In MEMAP, the field enhancement from a noble-metal nanostructure is used to reduce the exposure threshold of a photoresist. MEMAP has been demonstrated for a range of nanostructures, including rough gold surfaces,⁸ sharp metallic tips,²³ nanobowties,⁹ nanoparticle aggregates,¹⁰ nanorods,²⁴ and arrays of nanosquares.²⁵ It has often been assumed that MEMAP occurs because field enhancement leads to more efficient multiphoton excitation of the photoinitiator in the photoresist. However, we recently demonstrated that for nanoparticle aggregates, MEMAP could be driven equally efficiently even at wavelengths for which two-photon excitation of the photoinitiator was not possible.¹⁰ This result strongly suggests that, at least for that particular system, the dominant mechanism of MEMAP was single-photon excitation of the photoinitiator driven by MAIL.

Our goal here is to explore the mechanism of MEMAP and its connection to MAIL in greater detail by employing a different type of noble-metal nanostructure and different photoinitiators and photoresists. The gold nanoparticle aggregates that we examined previously were quite heterogeneous. Here we investigate gold nanowires, which have more reproducible structures. In addition, our previous study involved an acrylic photoresist with one particular photoinitiator, Lucirin TPO-L.²⁶ Here we examine the same resist with two other radical photoinitiators that differ substantially from Lucirin TPO-L. We also examine SU8, an epoxy photoresist that has been used in a number of previous studies of MEMAP.^{9,24,25} SU8 undergoes cationic polymerization rather than radical polymerization, and so uses a photoacid generator (PAG) rather than a radical photoinitiator. We find a strong correlation between MEMAP and MAIL in all of these systems, and based on wavelength-dependent studies, we demonstrate that the dominant mechanism of MEMAP is the same as was found previously for gold nanoparticle aggregates.¹⁰

II. Experimental Section

Nanowire Synthesis. Au nanowires were fabricated by the electrochemical deposition of Au in the pores of the anodized aluminum oxide (AAO) film as a template.^{27,28} AAO template

films with highly ordered hexagonal pore channel arrays were fabricated by the anodization of high purity (99.99%) Al foil under a potential of 40 V at 10 °C in 0.3 M oxalic acid for 24 h. Prior to the anodization, the Al foil was electropolished using a mixture of perchloric acid and ethanol. After anodization, the Al on the barrier side at the bottom of the pores was dissolved in a saturated mercury chloride solution until only a thin barrier layer remained. The barrier layer was etched and removed by the exposure to a 5% phosphoric acid solution at 30 °C in order to make a through-pore, free-standing AAO film. After 40 min of etching, the barrier layer is slightly opened and the AAO film pores begin to be widened. Further etching between 10 and 40 min completely opened the barrier and further widened the pores to the desired diameter (50 – 80 nm). A layer of Au (200 nm) was then sputtered on the barrier side of the AAO template film to ensure a good electrical contact. Ni was electrodeposited on the sputtered Au in the pores with 0.1 M NiCl₂ solution at −0.9 V vs Ag/AgCl in order to seal up the ends of the pores completely, and also to remove surface roughness associated with sputtered Au at the bottom of the pores. Au nanowires were electrodeposited at a constant current of 0.3 mA in the gold plating solution (Orotemp 24, Technic). The length of the gold nanowires can be controlled by the charge passed during the electrochemical deposition. Usually 1 C/cm² gives a gold segment with a length of about 1 μm. Nickel and gold depositions were repeated for the desired number of cycles. After the Au and Ni were grown alternately over a sufficient number of cycles, the sputtered Au layer was removed by mechanical polishing with sand paper. The AAO template was then removed with 3 M NaOH for 2 h. Nitric acid (3 M) was used to remove the Ni segments selectively. The freed Au nanowires were rinsed with deionized water and kept in ethanol.

Substrate Preparation. To promote adhesion of polymeric structures created with multiphoton absorption polymerization (MAP), glass coverslips were pretreated by immersion in a solution of 93 vol% ethanol, 5 vol% distilled water, and 2 vol% (3-acryloxypropyl) trimethoxysilane (95%, Gelest, Inc.) for 12 h. The coverslips were then rinsed in ethanol for 1 h and dried in an oven at 95 °C for 1 h.

In order to facilitate the identification of specific nanowires with scanning electron microscopy after MAIL and MEMAP experiments, MAP^{29–31} was used to write lines forming a 75 μm × 75 μm grid divided into 36 squares on the substrate. An acrylic resin composed of 54 wt % dipentaerythritol pentaacrylate esters (Sartomer), 43 wt % tris(2-hydroxyethyl) isocyanurate triacrylate (Sartomer), and 3 wt % Lucirin TPO-L (BASF) was used to fabricate the patterns.

MAP was performed using a tunable femtosecond Ti:sapphire oscillator (Coherent Mira 900-F). The repetition rate of the laser was 76 MHz and the pulse length was approximately 150 fs. Laser pulses (800 nm) with a power of 2.3 mW (all powers are measured at the sample) were focused through a 100×, 1.45 NA oil-immersion objective (Zeiss R Plan-FLUAR) on an inverted microscope (Zeiss Axiovert 100) to write the lines at a stage velocity of 20 μm/sec. After fabrication, the unexposed resin was rinsed in dimethylformamide two times for 3 min each, following by two rinses in ethanol for 3 min each.

Once patterned substrates had been prepared, one drop of a gold nanowire suspension was placed on the coverslip in the region with the pattern. The gold nanowire suspension was prepared by mixing approximately 200 μg of dried gold nanowires with 200 μL of distilled water. Sonication for 30 min dispersed the gold nanowires thoroughly in the distilled water, and a light pink suspension was obtained. To deposit

the gold nanowires on the patterned substrates, the distilled water was evaporated in an oven at 95 °C for 3 min.

Acrylic Photoresists for MEMAP. The acrylic photoresist was composed of 55 wt % dipentaerythritol pentaacrylate (Sartomer), 44 wt % tris (2-hydroxy ethyl) isocyanurate triacrylate (Sartomer), and 1 wt % of a radical photoinitiator. We tested two different radical photoinitiators, 2-benzyl-2-dimethylamino-1-(4-morpholinophenyl)-butanone-1 (Irgacure 369, Ciba) and 1-hydroxy cyclohexylphenylketone (Irgacure 184, Ciba). After thorough mixing, one drop of a prepolymer photoresist was placed on a substrate with gold nanowires. The sample was then covered with a coverslip using a layer of Scotch tape as a spacer.

For development after MEMAP experiments, samples were immersed in dimethylformamide for 3 min twice and then in ethanol for 3 min twice to remove any unpolymerized resin. After drying, samples were sputter-coated with 10 nm of Pt/Pd for SEM imaging.

SU8 photoresists for MEMAP. Commercial SU8 2000 Series resists (MicroChem) are composed of 23–96 wt % of cyclopentanone, 0.3–5 wt % of triarylsulfonium hexafluoroantimonate salts in propylene carbonate, and 3–75 wt % of epoxy resin.

SU8 with a low concentration of PAG was prepared as follows. Triarylsulfonium hexafluoroantimonate salts in propylene carbonate (0.006 g; 50%, Aldrich) was mixed with 1.5 g of cyclopentanone (99%, Fluka). The mixture was then further diluted to 0.01 wt % of PAG in cyclopentanone. EPON Resin SU8 (EPIKOTETM 157, Hexion) was ground into fine powder and blended with the mixture in a 1:1 weight ratio so that the final SU8 photoresist would contain 0.01 wt % PAG.

The mixture was dissolved completely after 4 h and was filtered twice through 200-nm pores. To render the SU8 photoresist viscous enough to be spread out as a film, the solution was heated in an oven at 95 °C for 5 min and then at 110 °C for 2 min. After repeating this evaporation process until three-fourths of the original volume remained, the sample was cooled to room temperature.

One droplet of SU8 photoresist was placed on a substrate with gold nanowires. Spinning at 4000 rpm for 1 min formed a 20-μm-thick film. The SU8 film was then placed in an oven to bake at 65 °C for 2 min, at 95 °C for 20 min, and then at 65 °C for 5 min. After this prebake, the sample was cooled to room temperature.

After MEMAP exposure, the SU8 film was postbaked by placing it in an oven at 65 °C for 2 min, at 95 °C for 20 min, and then 65 °C for 5 min. When the sample was cooled to room temperature, it was rinsed in SU-8 Developer (MicroChem) for 6 min two times, following by an isopropanol rinse for 3 min. After drying, the sample was sputter-coated with 10 nm of Pt/Pd for SEM imaging.

MAIL imaging and MEMAP. The laser described above was employed for the MAIL and MEMAP studies. The laser was tuned from 724 to 930 nm to cover the wavelength range used in the experiments. The objective and microscope are the same ones described above. Samples were mounted on a three-dimensional (3D) piezoelectric stage (P-562 PIMarsTM XYZ Piezo System, Physik Instrumente) for fine sample positioning in all dimensions. The piezo stage was attached to a motor-driven stage (Bioprecision, Ludl Electronic Products) for coarse sample positioning.

To capture the MAIL images, the beam was scanned over a sample using galvanometric mirrors. All luminescence signals were detected by a single-photon-counting avalanche photodiode

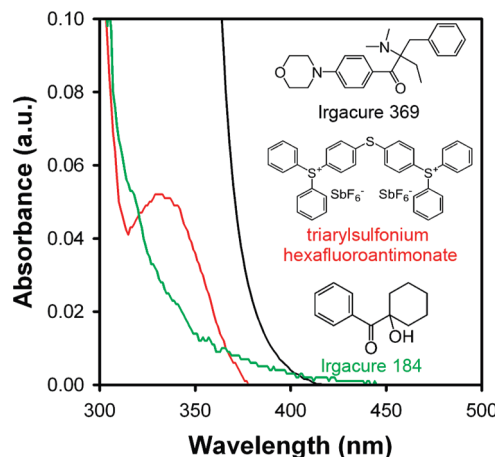


Figure 1. Linear absorption spectra of thin films of the photoresists used for MEMAP.

(EG&G) and transferred to a computer. Scanning of the sample and imaging of luminescence were controlled using programs written in LabView (National Instruments).

In typical MAIL and MEMAP experiments, the beam scanned an area of about $2.5 \mu\text{m}^2$ containing a single gold nanowire for 2 s with 88×88 pixel resolution. The scanning was repeated three times, and the MAIL signals were averaged. For samples with photoresists, MAIL and MEMAP were typically performed simultaneously. For samples without a photoresist, immersion oil (Immersol 518 F fluorescence free, Zeiss) was placed on the substrate to facilitate the identification of single gold nanowires for MAIL studies.

III. Results

The linear absorption spectra of thin films of the photoresists used in this study are shown in Figure 1, denoted by the relevant photoinitiator. The linear absorption of each radical photoinitiator cuts off before 450 nm, and the absorption of the PAG cuts off at about 375 nm. To determine the longest wavelength at which MAP is possible using two-photon absorption in the absence of metal nanowires, we performed wavelength-dependent studies up to the maximum laser power available (~ 12 mW; all reported laser powers are at the sample). For Irgacure 369 and Irgacure 184, MAP was not observed at any intensity at wavelengths of 890 nm and longer. However, for commercial SU8 we observed MAP at low laser powers (1.3 mW) even with the laser tuned to 930 nm. As can be seen from Figure 1, the linear absorption spectrum of the PAG used in SU8 has gone to baseline at wavelengths that are considerably less than 465 nm (which is half of 930 nm).

On the basis of the linear absorption spectrum of the PAG, it is surprising that MAP should be so efficient in SU8 at wavelengths as long as 930 nm. However, it should be kept in mind that the concentration of the PAG in commercial SU8 photoresists is on the order of 1 wt %. While this is a typical concentration for photopolymerization, it is high enough that some degree of aggregation is possible. Furthermore, the PAG is actually a mixture of the structure shown in Figure 1 and one in which one end of the molecule terminates in a phenyl group rather than a triarylsulfonium group. Highly polar species of this type may have a propensity to form aggregates of antiparallel molecules. In these so-called H-aggregates, the linear absorption spectrum shifts to the blue.³² However, for symmetry reasons a two-photon absorption spectrum of the aggregate can shift to the red.

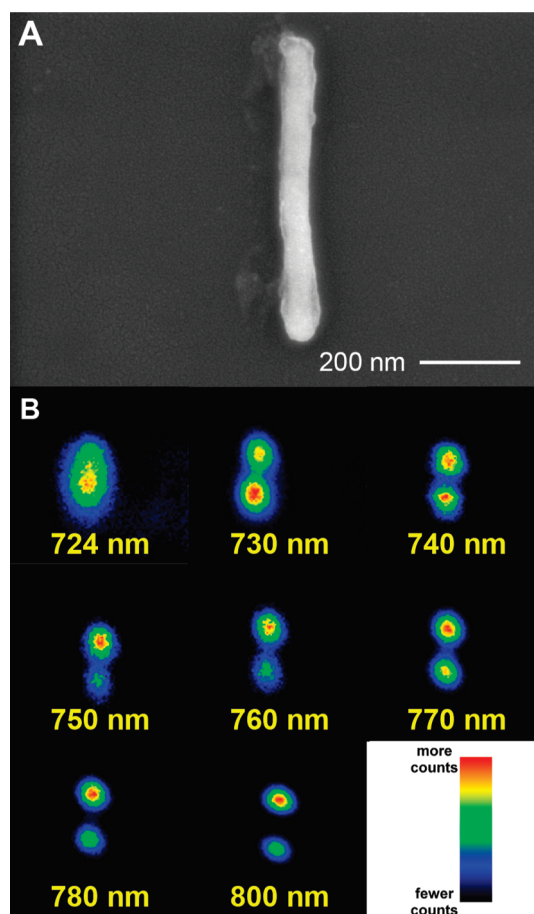


Figure 2. (A) SEM of a gold nanowire used for MAIL imaging. The thin coating at the ends of the wire arises from a photochemical reaction of the immersion oil used. (B) Normalized MAIL excitation images of this nanowire obtained at different laser wavelengths. The excitation power at each wavelength was 0.83 mW at the sample.

To test whether aggregation is responsible for our ability to perform MAP in SU8 at long wavelengths, we prepared our own SU8 with a lower concentration of PAG, as described above. With only 0.01 wt % of the PAG, we are unable to perform MAP at wavelengths longer than 800 nm. However, at high powers, we do observe laser-induced damage in the photoresist.

We next consider the wavelength dependence of MAIL for these nanowires. Shown in Figure 2 is a scanning electron micrograph (SEM) of a typical gold nanowire along with normalized MAIL excitation images (i.e., each image was scaled by its maximum intensity) obtained at different laser wavelengths at a constant excitation power of 0.83 mW. At shorter wavelengths, MAIL can be excited anywhere along the length of the wire. However, as the wavelength increases, MAIL excitation is efficient only at the ends of the nanowire. Furthermore, as shown in the unnormalized MAIL excitation images (i.e., no scaling was performed) in Figure 3, the MAIL excitation efficiency is strongest at the shortest and longest wavelengths, and decreases in between. This phenomenon may reflect stronger coupling into transverse plasmons at shorter wavelengths and into longitudinal plasmons at longer wavelengths. We have observed similar behavior for all isolated nanowires that we have studied.

We next consider the correlation between MAIL and MEMAP. Shown in Figure 4 are MAIL excitation images of two

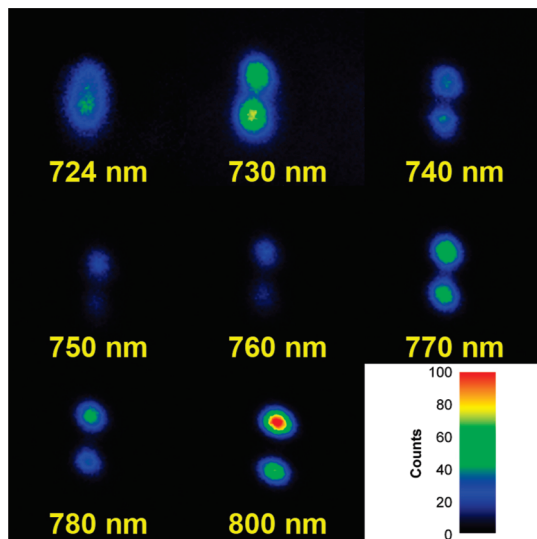


Figure 3. Unnormalized MAIL excitation images corresponding to the normalized MAIL excitation images in Figure 2.

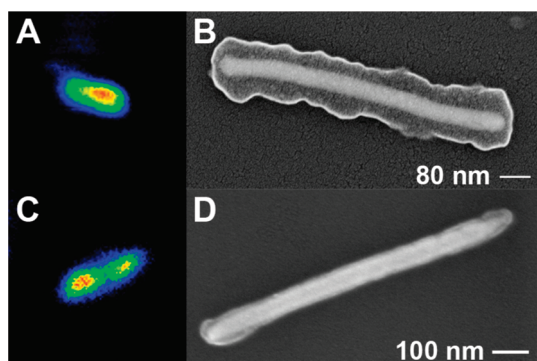


Figure 4. (A) MAIL excitation image of a nanowire excited with 730 nm light in an acrylic resin containing 1 wt % Irgacure 184. (B) SEM image of the nanowire from (A) after development. (C) MAIL excitation image of a nanowire excited with 740 nm light in an acrylic resin containing 1 wt % Irgacure 184. (D) SEM image of the nanowire from (C) after development.

nanowires in an acrylic photoresist with Irgacure 184 as the photoinitiator. The first nanowire (Figure 4A) was excited at 730 nm, and shows efficient excitation along its entire length. The second nanowire (Figure 4C) was excited at 740 nm, and the areas of efficient excitation are biased toward the ends of the nanowire. The accompanying SEM images of the nanowires after MEMAP show that the areas of polymerization are strongly correlated with the areas of efficient MAIL excitation. Similar behavior was observed for all nanowires studied, indicating that there is a strong correlation between MAIL and MEMAP.

To investigate the mechanism of MEMAP, we performed experiments with an excitation wavelength of 890 nm. Even at the highest powers available, MAP was not possible at this wavelength with any of the photoresists used here. It is therefore unlikely that MAP can be driven by two-photon absorption for any of these photoresists at 890 nm. However, MAIL in gold nanostructures can readily be driven by absorption of three or more 890-nm photons,^{7,10} leading to MAIL emission that extends into the UV region of the spectrum. Thus, if MEMAP occurs in these photoresists with 890-nm excitation, it is a strong indication that this process occurs not through enhanced two-photon excitation of the photoinitiator, but rather through single-photon excitation of the photoinitiator by MAIL emission.

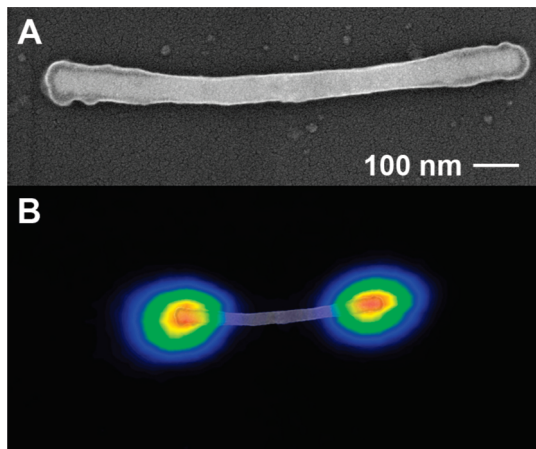


Figure 5. (A) SEM image of a nanowire that has undergone MEMAP in an acrylic resin with 1 wt % Irgacure 369 at an excitation wavelength of 890 nm. (B) MAIL excitation image of the nanowire from (A) obtained during the MEMAP exposure. An SEM image of the nanowire has been overlaid on the MAIL image.

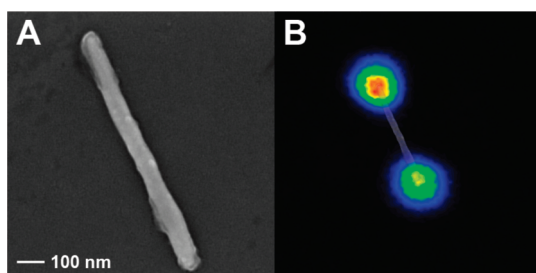


Figure 6. (A) SEM image of a nanowire that has undergone MEMAP in an acrylic resin with 1 wt % Irgacure 184 at an excitation wavelength of 890 nm. (B) MAIL excitation image of the nanowire from (A) obtained during the MEMAP exposure. An SEM image of the nanowire has been overlaid on the MAIL image.

Shown in Figure 5A is an SEM image of a gold nanowire that was scanned with 890-nm pulses at an average power of 4.1 mW while in an acrylic photoresist with Irgacure 369 as the photoinitiator. The MAIL excitation image obtained during exposure is shown in Figure 5B, along with a superimposed SEM image of the nanowire. The polymer coating is seen predominantly at the ends of the nanowire, and is strongly spatially correlated with the MAIL excitation image.

In Figure 6A we show an SEM image of a gold nanowire that was exposed to 890-nm pulses at an average power of 2.5 mW while in an acrylic photoresist with Irgacure 184 as the photoinitiator. Again, a polymer coating is observed at the ends of the nanowire. This coating is less prominent than for Irgacure 369, presumably because the MAIL emission of the nanowire has less overlap with the linear absorption spectrum of Irgacure 184 (see Figure 1). As can be seen in Figure 6B, again there is a strong correlation between the location of the polymer coating and the bright regions in the MAIL excitation image.

A gold nanowire that was exposed to 890-nm pulses at an average power of 3.3 mW while in SU8 with 0.01 wt % PAG is shown in Figure 7A. Once again the polymerization is highly localized to the ends of the wire. In SU8 the polymerized regions extend farther away from the wire than was the case for acrylic photoresists, which may result from diffusion of the acid generated during exposure in combination with local heating due to excitation of the nanowire. As can be seen from the

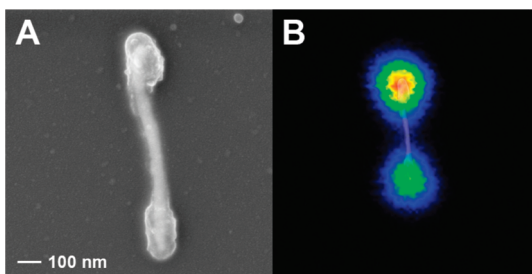


Figure 7. (A) SEM image of a nanowire that has undergone MEMAP in SU8 with 0.01 wt % PAG at an excitation wavelength of 890 nm. (B) MAIL excitation image of the nanowire from (A) obtained during the MEMAP exposure. An SEM image of the nanowire has been overlaid on the MAIL image.

MAIL excitation image in Figure 7B, there is once again a strong correlation between the spatial locations of MAIL and MEMAP.

IV. Discussion

We have previously studied the relationship between MAIL and MEMAP using clusters of gold nanoparticles.¹⁰ Those studies indicated that, for such aggregates, linear absorption of MAIL emission is the predominant mechanism of MEMAP. However, every nanoparticle aggregate is unique, and not all aggregates exhibit efficient MAIL and MEMAP.¹⁰ Thus, it is possible that there is a particular structural or physical feature that causes some aggregates to exhibit efficient MAIL, and that this same factor contributes to efficient MEMAP driven by the MAIL emission.

The gold nanowires studied here are much more uniform than are the gold nanoparticle aggregates we studied previously. In addition, the nanowires can be observed optically in a bright-field microscope. We are thus able to ascertain that all isolated nanowires have similar MAIL properties, allowing us to draw clear conclusions regarding the dominant mechanism of MEMAP.

MAP cannot be driven by two-photon excitation at 890 nm in any of the photoresists studied here. In fact, for SU8 the threshold for laser-induced damage at this wavelength is lower than the threshold for MAP. However, in all cases, MEMAP occurs efficiently at this wavelength and has a strong spatial correlation with MAIL excitation. This result indicates that, at long wavelengths, the dominant mechanism for MEMAP is linear absorption of MAIL emission. As there is no significant qualitative change in MEMAP behavior in moving to the shorter excitation wavelengths studied here, it appears likely that the dominant mechanism for MEMAP remains the same over the entire range of wavelengths studied here.

The fact that MEMAP appears to be driven predominantly by MAIL emission for every photoinitiator that we have studied (the three discussed here plus Lucirin TPO-L¹⁰) suggests that this is a highly general mechanism. Indeed, Diebold, Peng, and Mazur have also suggested that this mechanism holds in their experiments on a positive-tone photoresist on rough silver surfaces.¹¹ It will be interesting to investigate whether MAIL plays a role in other processes that depend upon field enhancement at noble-metal nanostructures. For instance, processes that involve emission, such as SERS, have maximum efficiencies that have not yet been able to be described adequately by theory. On the other hand, for processes that depend only on absorption, such as SEIRA, the observed enhancement matches well with theoretical predictions.

V. Conclusions

We have demonstrated that there is a strong spatial correlation between MAIL and MEMAP for gold nanowires excited at wavelengths ranging from 730 to 890 nm. Experiments performed at long wavelengths indicate that for all of the photoresists studied here, MEMAP is driven predominantly by linear absorption of MAIL emission. Our data also suggest that the same mechanism dominates at shorter wavelengths. We plan to pursue experiments on other types of noble-metal nanostructures to explore the generality of this mechanism for MEMAP.

Acknowledgment. We appreciate the support of the Maryland NanoCenter and its NispLab. The NispLab is supported in part by the NSF as a MRSEC Shared Experimental Facility. This work was supported in part by the UMD-NSF-MRSEC under Grant DMR 05-20471. S.B.L. was also supported by the WCU program through the KOSEF funded by the MEST (Grant Number R31-2008-000-10071-0).

References and Notes

- Bell, S. E. J.; Sirimuthu, N. M. S. *Chem. Soc. Rev.* **2008**, *37*, 1012.
- Tian, Z. Q.; Ren, B.; Wu, D. Y. *J. Phys. Chem. B* **2002**, *106*, 9463.
- Lal, S.; Grady, N. K.; Kundu, J.; Levin, C. S.; Lassiter, J. B.; Halas, N. J. *Chem. Soc. Rev.* **2008**, *37*, 898.
- Goutev, N.; Futamata, M. *Appl. Spectrosc.* **2003**, *57*, 506.
- Osawa, M. Surface-Enhanced Infrared Absorption. In *Near-Field Optics and Surface Plasmon Polaritons*; Kawata, S., Ed.; Springer-Verlag: Berlin, 2001; Vol. 81, p 163.
- Boyd, G. T.; Yu, Z. H.; Shen, Y. R. *Phys. Rev. B* **1986**, *33*, 7923.
- Farrer, R. A.; Butterfield, F. L.; Chen, V. W.; Fourkas, J. T. *Nano Lett.* **2005**, *5*, 1139.
- Postnikova, B. J.; Currie, J.; Doyle, T.; Hanes, R. E.; Anslyn, E. V.; Shear, J. B.; Vanden Bout, D. E. *Microelectron. Eng.* **2003**, *69*, 459.
- Sundaramurthy, A.; Schuck, P. J.; Conley, N. R.; Fromm, D. P.; Kino, G. S.; Moerner, W. E. *Nano Lett.* **2006**, *6*, 355.
- Nah, S.; Li, L.; Fourkas, J. T. *J. Phys. Chem. A* **2009**, *113*, 4416.
- Diebold, E. D.; Peng, P.; Mazur, E. *J. Am. Chem. Soc.* **2009**, *131*, 16356.
- Beversluis, M. R.; Bouhelier, A.; Novotny, L. *Phys. Rev. E* **2003**, *68*, 115433.
- Kempa, T.; Farrer, R. A.; Giersig, M.; Fourkas, J. T. *Plasmonics* **2006**, *1*, 45.
- Eichelbaum, M.; Schmidt, B. E.; Ibrahim, H.; Rademann, K. *Nanotechnology* **2007**, *18*, 355702.
- Imura, K.; Nagahara, T.; Okamoto, H. *J. Phys. Chem. B* **2005**, *109*, 13214.
- Wang, D.-S.; Hsu, F.-Y.; Lin, C.-W. *Opt. Express* **2009**, *17*, 11350.
- Biagioli, P.; Celebrano, M.; Savoini, M.; Grancini, G.; Brida, D.; Mátéfi-Tempfli, S.; Mátéfi-Tempfli, M.; Duò, L.; Hecht, B.; Cerullo, G.; Finazzi, M. *Phys. Rev. B* **2009**, *80*, 045411.
- Gong, H. M.; Zhou, Z. K.; Xiao, S.; Su, X. R.; Wang, Q. Q. *Plasmonics* **2008**, *3*, 59.
- Park, J.; Estrada, A.; Sharp, K.; Sang, K.; Schwartz, J. A.; Smith, D. K.; Coleman, C.; Payne, J. D.; Korgel, B. A.; Dunn, A. K.; Tunnell, J. W. *Opt. Express* **2008**, *16*, 1590.
- Imura, K.; Nagahara, T.; Okamoto, H. *Appl. Phys. Lett.* **2006**, *88*, 023104.
- Durr, N. J.; Larson, T.; Smith, D. K.; Korgel, B. A.; Sokolov, K.; Ben-Yakar, A. *Nano Lett.* **2007**, *7*, 941.
- Wang, H. F.; Huff, T. B.; Zweifel, D. A.; He, W.; Low, P. S.; Wei, A.; Cheng, J. X. *Proc. Natl. Acad. Sci. U.S.A.* **2005**, *102*, 15752.
- Yin, X.; Fang, N.; Zhang, X.; Martini, I. B.; Schwartz, B. J. Near-Field Multiphoton Nanolithography Using an Apertureless Optical Probe. In *Nonlinear Optical Transmission and Multiphoton Processes in Organics*; Yeates, A. T., Belfield, K. D., Kajzar, F., Lawson, C. M., Eds.; SPIE: Bellingham, WA, 2003; pp 96.
- Murazawa, N.; Ueno, K.; Mizeikis, V.; Juodkazis, S.; Misawa, H. *J. Phys. Chem. C* **2009**, *113*, 1147.
- Ueno, K.; Juodkazis, S.; Shibuya, T.; Mizeikis, V.; Yokota, Y.; Misawa, H. *J. Phys. Chem. C* **2009**, *113*, 11720.
- Baldacchini, T.; LaFratta, C.; Farrer, R. A.; Teich, M. C.; Saleh, B. E. A.; Naughton, M. J.; Fourkas, J. T. *J. Appl. Phys.* **2004**, *95*, 6072.
- Liu, R.; Lee, S. B. *J. Am. Chem. Soc.* **2008**, *130*, 2942.

- (28) Xiao, R.; Il Cho, S.; Liu, R.; Lee, S. B. *J. Am. Chem. Soc.* **2007**, *129*, 4483.
- (29) LaFratta, C. N.; Fourkas, J. T.; Baldacchini, T.; Farrer, R. A. *Angew. Chem., Int. Ed.* **2007**, *46*, 6238.
- (30) Maruo, S.; Fourkas, J. T. *Laser Photon. Rev.* **2008**, *2*, 100.
- (31) Rumi, M.; Barlow, S.; Wang, J.; Perry, J. W.; Marder, S. R. Two-Photon Absorbing Materials and Two-Photon-Induced Chemistry. In

Photoresponsive Polymers I; Marder, S., Neher, D., Eds.; Springer-Verlag: Berlin, 2008; Vol. 213, p 1.

(32) Pengchong, X.; Ran, L.; Xinchun, Y.; Li, Z.; Defang, X.; Yan, L.; Hanzhuang, Z.; Hiroyuki, N.; Makoto, T.; Hirotaka, I. *Chem.—Eur. J.* **2009**, *15*, 9824.

JP100387K